Junctions and Superconducting Symmetry in Twisted Bilayer Graphene

Héctor Sainz-Cruz,[1,*] Pierre A. Pantaleón,[1] Võ Tiến Phong,[2] Alejandro Jimeno-Pozo,[1] and Francisco Guinea[1,3]
[1]Imdea Nanoscience, Faraday 9, 28015 Madrid, Spain
[2]Department of Physics and Astronomy, University of Pennsylvania, Philadelphia, Pennsylvania 19104, USA
[3]Donostia International Physics Center, Paseo Manuel de Lardizabal 4, 20018 San Sebastian, Spain

(Received 22 November 2022; accepted 31 May 2023; published 7 July 2023; corrected 18 July 2024)

Junctions provide a wealth of information on the symmetry of the order parameter of superconductors. We analyze junctions between a scanning tunneling microscope (STM) tip and superconducting twisted bilayer graphene (TBG) and TBG Josephson junctions (JJs). We compare superconducting phases that are even or odd under valley exchange (s- or f-wave). The critical current in mixed (s and f) JJs strongly depends on the angle between the junction and the lattice. In STM-TBG junctions, due to Andreev reflection, the f-wave leads to a prominent peak in subgap conductance, as seen in experiments.

DOI: 10.1103/PhysRevLett.131.016003

Introduction.—Graphene multilayers host a myriad of exotic correlated and topological phases [1–23]. Perhaps most interesting and enigmatic among them is superconductivity, possibly with unconventional pairing symmetries and mechanisms, observed in alternating-twist stacks of up to five layers [24–30] and in Bernal bilayers and rhombohedral trilayers [31–34]. Crucially, the observed superconductivity violates the Pauli limit for spin-singlet pairing [29,31–35] and has been observed in settings that break time-reversal symmetry (TRS) [36], strongly suggesting a spin-triplet pairing in these materials. However, the pairing may be a mixture of singlet and triplet [37], and the exact symmetries involved (s, p, d, and/or f) are still unknown despite intense theoretical and experimental efforts to uncover them.

Recently, several experiments have studied these unconventional superconducting states using transport measurements: either with a scanning tunneling microscope (STM) tip [16,22] or with Josephson junctions (JJs) [38–42] and superconducting quantum interference devices (SQUIDs) [43]. In the former setup, by comparing the transmission between the STM tip and the superconducting surface in the weak and strong-coupling regimes, one can gain important insights about the symmetry of the order parameter. For instance, the experimental observations, such as the peak in the subgap conductance [16,22], seem inconsistent with s-, p- and d-wave pairings [37,44]. In the latter setups, the overlap of the superconductors' wave functions at the junction's link gives rise to a zero-frequency supercurrent whose magnitude and superconducting phase-dependence carry characteristics of the pairing symmetry [45–47].

Building on these experimental insights, we argue in this Letter that transport measurements in junctions are ideal probes of the pairing symmetry in twisted graphene superconductors, similar to the elucidation of d-wave pairing in cuprate superconductors [48,49], and that existing STM data [16,22] are consistent with f-wave pairing. The Fermi surface of these graphene-based systems contains two valleys. We consider superconducting order parameters that are either even or odd under valley exchange, which in the absence of spin-orbit coupling correspond to spin-singlet s-wave superconductivity or spin-triplet f-wave superconductivity, respectively. In "mixed" Josephson junctions connecting a s-wave to a f-wave superconductor, we observe that the critical current dramatically depends on the angle between the junction and the graphene lattice axis. Therefore, Josephson junctions are useful for determining whether two superconducting phases differ in their valley exchange parity.

In the STM-superconductor junction, we find that the subgap conductance shows a prominent zero-bias peak for f-wave pairing only, due to enhanced Andreev reflection. This peak has been observed in experiments on both twisted bilayer [16] and twisted trilayer graphene [22]. This result puts forward f-wave pairing as a leading candidate for the superconducting symmetry of twisted bilayer graphene, which is also consistent with previous theoretical models based on Coulomb-interaction-mediated Cooper pairing [50,51].

STM tip-superconducting TBG junction. The model.—General features of transport in normal-superconductor junctions are described in Ref. [52]. The coupling between the two electrodes is given by a scattering matrix, determined by a dimensionless transmission amplitude, T. The model has been extended in [37,44]. As in Ref. [52], the normal metal tip and the superconducting electrode are described in terms of incoming and outgoing single channels. On the superconductor, the states in the channel are defined as suitable averages in momentum space of the quasiparticles. The momentum dependence of the gap leads to a momentum dependence of the mixing between electron

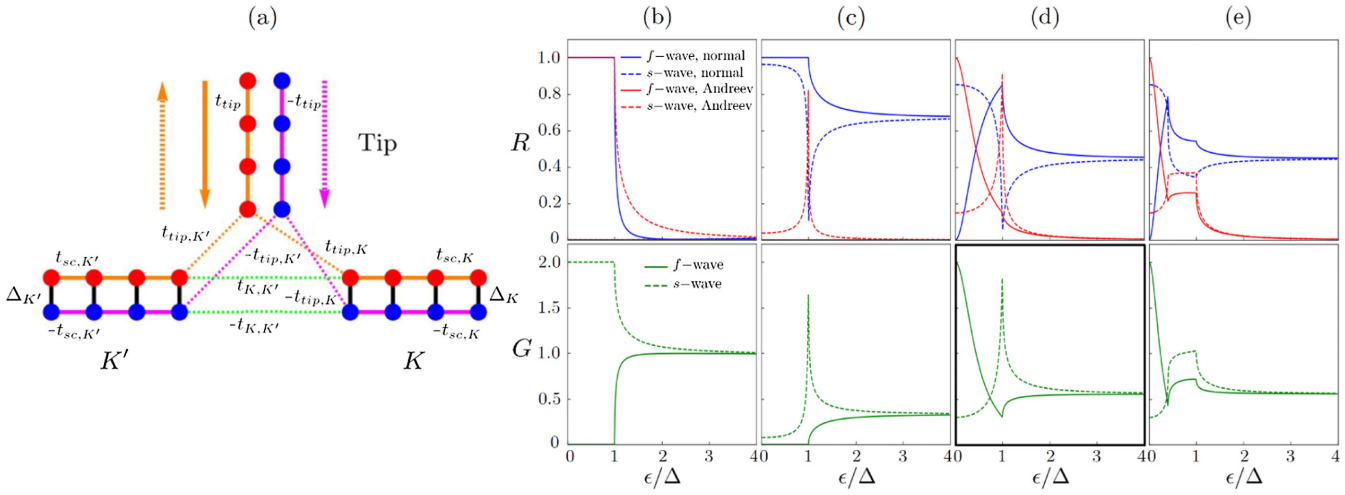

FIG. 1. STM tip-superconducting TBG junction. (a) Sketch of the model for the junction used to calculate its transport properties. See text for details. (b)–(e) Normal and Andreev reflections (top) and total conductance (bottom) for junctions with spin-singlet s-wave (dashed) and spin-triplet f-wave pairing (solid), in the perfect contact limit. (b) With equal Fermi velocities in all channels, $t_{\rm tip} = t_{sc,K} = t_{sc,K'} = 1$, $t_{{\rm tip},K} = t_{{\rm tip},K'} = 1/\sqrt{2}$, $t_{K,K'} = 0$, $\Delta_K = 0.05$, $\Delta_{K'} = \pm 0.05$. (c) With a large Fermi velocity mismatch in the normal and superconducting channels: $t_{\rm tip} = 10$, $t_{{\rm tip},K} = t_{{\rm tip},K'} = 10/\sqrt{2}$, others as in (b). (d) With Fermi velocity mismatch and intervalley scattering $t_{K,K'} = 1$, others as in (c). (e) With Fermi velocity mismatch, intervalley scattering and spin-orbit coupling: $\Delta_K = 0.05$, $\Delta_{K'} = \pm 0.02$, others as in (d).

and holelike states in the superconductor, and it modifies the transmission of the junction, both in the tunneling and in the contact regimes. The Blonder-Tinkham-Klapwijk (BTK) model [52] has also been extended to strongly coupled superconductors, where the chemical potential can be below the bottom of the band [53,54].

We describe the metal-superconductor junction as one ingoing normal channel, which represents the tip, and two outgoing superconducting channels, which represent the two valleys in TBG. The signs of the gaps in these channels can be equal, describing a spin-singlet s-wave superconductor, or opposite, describing a spin-triplet f-wave superconductor [55]. The model can also be applied to an Ising superconductor [34] in a system with strong spin-orbit coupling, characterized by spin-valley locked Cooper pairs of the type $|K,\uparrow;K',\downarrow\rangle$.

The three-channel model described above is discretized as a tight-binding model, see Fig. 1(a). The normal channel is described by nearest-neighbor hopping $t_{\rm tip}$, which determines its Fermi velocity and density of states. The superconducting channels are described by two nearest neighbor hoppings, $t_{sc,K}$ and $t_{sc,K'}$, and two gaps, Δ_K and $\Delta_{K'}$. The coupling between the normal channel and the two superconducting channels is described by the hoppings $t_{{\rm tip},K}$ and $t_{{\rm tip},K'}$. Without loss of generality, we assume that the Fermi energy is $\epsilon_F = 0$, so that each channel has exact electron-hole symmetry. Finally, we consider that the tip is a local perturbation which can induce intervalley scattering, parametrized by another hopping, $t_{K,K'}$.

We solve the transmission of the junction by matching incoming and outgoing waves in the three channels. If the energy ϵ is within the superconducting gaps, we use evanescent waves in the superconducting channels. For each energy, there are four propagating or evanescent waves in each channel. We assume that there is an incoming wave of electron character and amplitude 1 in the tip channel. In the same channel, there can be one electron and one hole outgoing channels, describing normal and Andreev reflection, with amplitudes R_N and R_A, respectively. In each of the two superconducting channels there can be two decaying evanescent waves, when the energy is within the gap, or two outgoing propagating waves. We describe the four amplitudes as $T_{i,j}$, where $i = K, K'$ stands for the channel, and $j = 1, 2$ stands for the wave function within each channel. The transport properties of the junction are determined by these six amplitudes. The conductance of the junction is $G = 1 - |R_N|^2 + |R_A|^2$. The matching conditions involve the amplitudes of the wave functions at the three sites which describe the junction. The equations can be found in Ref. [56].

STM tip-superconducting TBG junction. Results.— When the Fermi velocities in all channels are equal, the tip channel merges smoothly into the even combination of the K and K' channels and the junction behaves as described by the BTK theory in the regime of perfect contact, see Fig. 1(b). For s-wave pairing, and at zero voltage, Andreev scattering leads to a conductance twice as large as a single normal channel [52]. For f-wave pairing, negative interference between the two hole channels

cancels Andreev reflection. This cancellation can be expected whenever the order parameter has a sign change between states related by TRS [44]. At high voltages the conductance reduces to the conductance of a single channel in both cases.

The bandwidth and Fermi velocity in TBG are considerably smaller than in a normal metal. This Fermi velocity mismatch induces elastic backscattering in the normal phase, which reduces the conductance above the gap, see Fig. 1(c). Subgap Andreev reflection for s-wave superconductivity is strongly suppressed, and it remains zero for the f-wave phase, for a detailed explanation see Ref. [56]. The tip can also induce a perturbation on the superconductor, on scales comparable to the atomic spacing. Such a perturbation will induce intervalley scattering. Figure 1(d) shows results obtained for an intervalley coupling comparable to the bandwidth of the superconductor. This perturbation can be considered as disorder, which does not violate TRS. The presence of intervalley scattering does not change significantly the conductance of the junction in an s-wave superconductor, in agreement with Anderson's theorem [62]. On the other hand, it is a pair breaking perturbation in an f-wave superconductor which induces subgap states, see Ref. [56]. These states allow for subgap Andreev reflection. As a result, the subgap conductance of the junction is strongly enhanced by intervalley scattering in an f-wave superconductor, leading to a zero bias peak, highlighted in Fig. 1(d), that has been seen in the experiments of Refs. [16,22].

Recent transport experiments [33,34] reveal that proximity induced spin-orbit coupling promotes the superconducting properties of Bernal bilayer graphene. An effect of spin-orbit coupling is to break the equivalence between the Cooper pairs $|K,\uparrow;K',\downarrow\rangle$ and $|K,\downarrow;K'\uparrow\rangle$. In the model studied here, the spin-orbit coupling makes the two channels inequivalent. Results are shown in Fig. 1(e).

Josephson junctions. The model.—For the study of JJs, our setup consists of a TBG crystal, in which the electrodes are superconducting and the weak link is in a normal metal or band insulating phase, as shown in Fig. 2(c). We start from a tight-binding, noninteracting Hamiltonian $\mathcal{H}_0$ [63] that includes Hartree electron-electron interactions through an electrostatic potential [64,65]. The parameters in the tight binding model are scaled, such that the central bands of a TBG with twist angle θ are approximated by the central bands of an equivalent lattice with twist angle $\lambda\theta$, with $\lambda > 1$ [66–68], see Fig. 2(a).

The critical current comes from second-order perturbation theory and is the derivative of the free energy E with respect to the superconducting phase difference ϕ:

$$\mathcal{I} = \frac{e}{h}\frac{\partial E}{\partial \phi}. \tag{1}$$

To obtain the energies of the TBG junction, we diagonalize the Bogoliubov–de Gennes Hamiltonian,

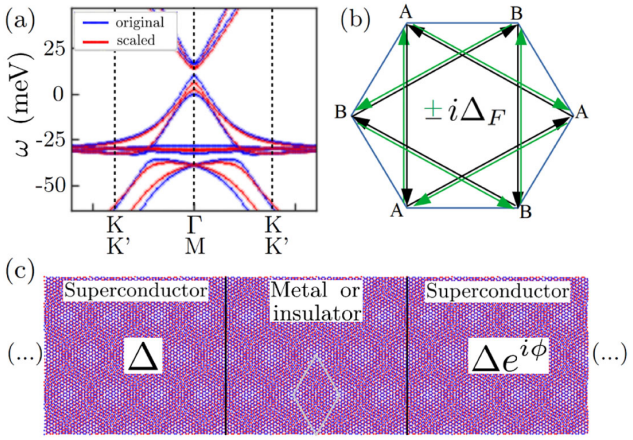

FIG. 2. (a) Low-energy band structure of TBG at $\theta \approx 1.08°$ and filling $n = -2.4$, with and without scaling. (b) Hoppings inducing f-wave superconducting pairing. (c) Central part of the lattice of the TBG Josephson junction [69,70]. The electrodes are superconductors with a phase difference of ϕ and the link region, with a length of four moiré periods, is metallic or insulating. The rhombus is a unit cell of TBG.

$$\mathcal{H}_{\mathrm{BdG}}|\Psi\rangle = \begin{pmatrix} \mathcal{H}_0 - \epsilon_F & f(\Delta) \\ f^\dagger(\Delta) & \epsilon_F - \mathcal{H}_0 \end{pmatrix}\begin{pmatrix} \Psi_e \\ \Psi_h \end{pmatrix} = E\begin{pmatrix} \Psi_e \\ \Psi_h \end{pmatrix}, \tag{2}$$

where ϵ_F is the Fermi energy. Again, we compare s-wave pairing, which we model with an on-site attractive Hubbard term $f(\Delta) = -\Delta_S \mathbb{1}$, and f-wave pairing, which results from Haldane-like hoppings [71,72] that allow an electron excitation to convert to a hole excitation via second nearest-neighbor imaginary intralayer hoppings, see Fig. 2(b).

Josephson junctions. Results.—Figure 3(a) compares the current-phase relations (CPRs) of TBG JJs with s- and f-wave pairings in multiple configurations. CPRs can be measured with a SQUID geometry [43]. The main message of Fig. 3 is that the type of pairing, s-wave or f-wave, plays a minor role when both electrodes are equal, compare dashed and solid lines in Figs. 3(a)–3(b).

In SNS JJs the CPR is skewed, due to high transmission of Andreev bound states, which carry over 80% of the current in these junctions and are mostly localized in AA stacking regions, see Fig. 3(c). In contrast, in SIS junctions the current comes from tunneling states, so the CPR is sinusoidal [74]. An exception occurs when the insulating gap in the link is comparable to the superconducting gap, resulting in skewness and large currents. The current in SIS junctions exponentially depends on the similitude between both gaps, see Fig. 3(d). We note that the authors of Ref. [43] report a sinusoidal CPR in TBG, without skewness, despite having a SNS JJ. This may be due to low transmission in the junction [47]. Figure 3(b) shows the critical current for all JJs as a function of twist angle. For a comparison to experiments, see Ref. [56]. The current in SNS JJs increases with twist angle, suggesting that larger

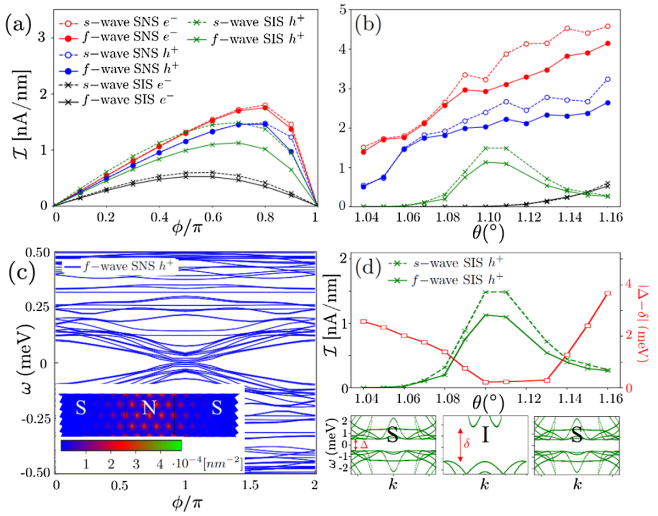

FIG. 3. TBG Josephson junctions with equal electrodes. (a) Current-phase relations for near magic-angle junctions with different pairing symmetry: spin-singlet s-wave (dashed) or spin-triplet f-wave (solid), for electron and hole superconducting domes (fillings $n = \pm 2.4$), with a metallic (SNS) or insulating link (SIS) [73] We set the superconducting gap to 1 meV [16]. $\theta = 1.06°$ for SNS; 1.1° for SIS h^+ and 1.16° for SIS e^-. Units: nanoampere per nanometer junction width. (b) Critical current versus twist angle for all configurations. (c) Andreev spectrum at 1.06°. Inset: charge map of an Andreev bound state. (d) Critical current in SIS JJs compared to the difference between the superconducting and insulating gaps, as a function of twist angle, and a sketch of the bands in the different regions of a SIS junction.

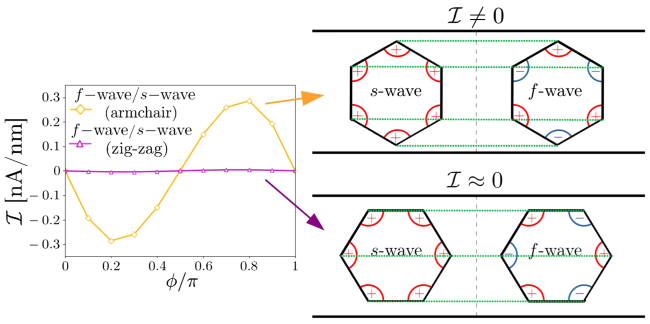

FIG. 4. Current-phase relation in mixed f-wave and s-wave TBG Josephson junctions, nearly parallel to the graphene armchair, as in Fig. 2(c), or zigzag directions. The critical current is ~100 times larger for armchair junctions.

Fermi velocities compensate the reduced density of states. Electron-hole asymmetry is very notable, e.g., near $\theta = 1.1°$, the current in SIS junctions with fillings $-2.4/4/-2.4$ is over 2 orders of magnitude larger than with $2.4/-4/2.4$ due to the asymmetry in the size of the gaps between narrow bands and electronlike or holelike remote bands.

Reference [38] reports a significant length dependence of the critical current in JJs prepared in mixed configurations, e.g., with the electrodes doped near one superconducting dome and the link near the other. This indicates that the superconducting pairing symmetry in the electron and hole domes may differ. The results in Fig. 4 for mixed f-wave and s-wave TBG JJs propose an experiment that could verify the hypothesis. For these JJs, the critical current dramatically depends on the angle between the junction and the lattice. A similar result in nonsuperconducting junctions was found in Ref. [75]. The critical current is sizable when the junction axis is nearly parallel to the graphene armchair direction, but close to zero when parallel to the zigzag direction. As long as the perpendicular momentum is conserved, the zigzag JJ suffers destructive interference of the superconducting pockets along the green lines drawn in Fig. 4. Also, the CPRs have a period of π, half the one of standard JJs. The origin of this effect is the existence of two sets of energy levels, due to coupling of the s-wave pocket to the two f-wave pockets, which have an intrinsic phase difference of π [46,76]. Furthermore, the CPR shows a π-junction behavior, i.e., it is first negative [47,77]. A requisite for these phenomena is that the triplet electrode is spin unpolarized, otherwise the current is zero due to spin conservation. The same occurs in a one-dimensional toy model [56,78].

Discussion.—We have studied the role of the superconducting order parameter in transport through superconducting TBG junctions. We focus on s- and f-wave pairing (even and odd valley combinations), as these two choices are equally favored by long range interactions, either attractive or repulsive [79].

We have calculated the critical current, and the current-phase relation for different types of Josephson junctions. JJs in which both electrodes are either s- or f-wave superconductors show similar features (unlike the s and p cases considered in Ref. [80]). On the other hand, the critical current in mixed (s and f) junctions depends strongly on the orientation of the junction with respect to the graphene lattice axes, with maxima for armchair junctions, and zeroes for zigzag junctions. Hence, mixed junctions are useful for determining whether two superconducting phases differ in their valley exchange parity. Such junctions can exist in various setups: (i) different superconducting regions in the phase diagram of TBG show different order parameters [38], (ii) the superconducting state changes locally because of the spin-orbit coupling induced by a substrate [33], (iii) superconducting TBG is combined with s-wave proximitized graphene [81,82].

For a junction between a normal STM tip and superconducting TBG, we find a prominent peak in subgap conductance for an f-wave order parameter, due to Andreev states induced by the tip, in agreement with the experiments of Refs. [16,22]. f-wave is also consistent with the U- and V-shaped densities of states measured in the weak coupling regime, as shown in Refs. [56,83]. The agreement between the experiments [16,22] and the results

presented here puts forward f-wave pairing as a leading candidate for the pairing symmetry of twisted graphene superconductors.

We note that the results for the STM-superconductor junction apply equally well to all graphene superconductors [27–34]. Extending the Josephson junction calculations to nontwisted graphene superconductors [31–34] is a promising direction for future research.

We thank Tommaso Cea, Shuichi Iwakiri, Klaus Ensslin, and Fernando de Juan for fruitful discussions. This work was supported by funding from the European Commission, within the Graphene Flagship, Core 3, Grant No. 881603; the Severo Ochoa programme for centres of excellence in R&D (CEX2020-001039-S/AEI/10.13039/501100011033) and grants SprQuMat (Ministerio de Ciencia e Innovación, Spain) and NMAT2D (Comunidad de Madrid, Spain). V. T. P. acknowledges support from the Department of Energy under Grant No. DE-FG02-84ER45118, the NSF Graduate Research Fellowships Program, and the P. D. Soros Fellowship for New Americans.

*hector.sainz@imdea.org

[1] Yuan Cao, Valla Fatemi, Ahmet Demir, Shiang Fang, Spencer L. Tomarken, Jason Y. Luo, Javier D. Sanchez-Yamagishi, Kenji Watanabe, Takashi Taniguchi, Efthimios Kaxiras, Ray C. Ashoori, and Pablo Jarillo-Herrero, Correlated insulator behaviour at half-filling in magic-angle graphene superlattices, Nature (London) **556**, 80 (2018).

[2] Hryhoriy Polshyn, Matthew Yankowitz, Shaowen Chen, Yuxuan Zhang, K. Watanabe, T. Taniguchi, Cory R. Dean, and Andrea F. Young, Large linear-in-temperature resistivity in twisted bilayer graphene, Nat. Phys. **15**, 1011 (2019).

[3] Aaron L. Sharpe, Eli J. Fox, Arthur W. Barnard, Joe Finney, Kenji Watanabe, Takashi Taniguchi, M. A. Kastner, and David Goldhaber-Gordon, Emergent ferromagnetism near three-quarters filling in twisted bilayer graphene, Science **365**, 605 (2019).

[4] M. Serlin, C. L. Tschirhart, H. Polshyn, Y. Zhang, J. Zhu, K. Watanabe, T. Taniguchi, L. Balents, and A. F. Young, Intrinsic quantized anomalous Hall effect in a moiré heterostructure, Science **367**, 900 (2020).

[5] Guorui Chen, Aaron L. Sharpe, Eli J. Fox, Ya-Hui Zhang, Shaoxin Wang, Lili Jiang, Bosai Lyu, Hongyuan Li, Kenji Watanabe, Takashi Taniguchi, Zhiwen Shi, T. Senthil, David Goldhaber-Gordon, Yuanbo Zhang, and Feng Wang, Tunable correlated Chern insulator and ferromagnetism in a moiré superlattice, Nature (London) **579**, 56 (2020).

[6] A. Uri, S. Grover, Y. Cao, J. A. Crosse, K. Bagani, D. Rodan-Legrain, Y. Myasoedov, K. Watanabe, T. Taniguchi, P. Moon, M. Koshino, P. Jarillo-Herrero, and E. Zeldov, Mapping the twist-angle disorder and Landau levels in magic-angle graphene, Nature (London) **581**, 47 (2020).

[7] Yu Saito, Jingyuan Ge, Kenji Watanabe, Takashi Taniguchi, and Andrea F. Young, Independent superconductors and correlated insulators in twisted bilayer graphene, Nat. Phys. **16**, 926 (2020).

[8] Dillon Wong, Kevin P. Nuckolls, Myungchul Oh, Biao Lian, Yonglong Xie, Sangjun Jeon, Kenji Watanabe, Takashi Taniguchi, B. Andrei Bernevig, and Ali Yazdani, Cascade of electronic transitions in magic-angle twisted bilayer graphene, Nature (London) **582**, 198 (2020).

[9] U. Zondiner, A. Rozen, D. Rodan-Legrain, Y. Cao, R. Queiroz, T. Taniguchi, K. Watanabe, Y. Oreg, F. von Oppen, Ady Stern, E. Berg, P. Jarillo-Herrero, and S. Ilani, Cascade of phase transitions and dirac revivals in magic-angle graphene, Nature (London) **582**, 203 (2020).

[10] Petr Stepanov, Ipsita Das, Xiaobo Lu, Ali Fahimniya, Kenji Watanabe, Takashi Taniguchi, Frank H. L. Koppens, Johannes Lischner, Leonid Levitov, and Dmitri K. Efetov, Untying the insulating and superconducting orders in magic-angle graphene, Nature (London) **583**, 375 (2020).

[11] Yang Xu, Song Liu, Daniel A. Rhodes, Kenji Watanabe, Takashi Taniguchi, James Hone, Veit Elser, Kin Fai Mak, and Jie Shan, Correlated insulating states at fractional fillings of moiré superlattices, Nature (London) **587**, 214 (2020).

[12] Youngjoon Choi, Hyunjin Kim, Yang Peng, Alex Thomson, Cyprian Lewandowski, Robert Polski, Yiran Zhang, Harpreet Singh Arora, Kenji Watanabe, Takashi Taniguchi, Jason Alicea, and Stevan Nadj-Perge, Correlation-driven topological phases in magic-angle twisted bilayer graphene, Nature (London) **589**, 536 (2021).

[13] Asaf Rozen, Jeong Min Park, Uri Zondiner, Yuan Cao, Daniel Rodan-Legrain, Takashi Taniguchi, Kenji Watanabe, Yuval Oreg, Ady Stern, Erez Berg, Pablo Jarillo-Herrero, and Shahal Ilani, Entropic evidence for a Pomeranchuk effect in magic-angle graphene, Nature (London) **592**, 214 (2021).

[14] Yuan Cao, Daniel Rodan-Legrain, Jeong Min Park, Noah F. Q. Yuan, Kenji Watanabe, Takashi Taniguchi, Rafael M. Fernandes, Liang Fu, and Pablo Jarillo-Herrero, Nematicity and competing orders in superconducting magic-angle graphene, Science **372**, 264 (2021).

[15] Petr Stepanov, Ming Xie, Takashi Taniguchi, Kenji Watanabe, Xiaobo Lu, Allan H. MacDonald, B. Andrei Bernevig, and Dmitri K. Efetov, Competing Zero-Field Chern Insulators in Superconducting Twisted Bilayer Graphene, Phys. Rev. Lett. **127**, 197701 (2021).

[16] Myungchul Oh, Kevin P. Nuckolls, Dillon Wong, Ryan L. Lee, Xiaomeng Liu, Kenji Watanabe, Takashi Taniguchi, and Ali Yazdani, Evidence for unconventional superconductivity in twisted bilayer graphene, Nature (London) **600**, 240 (2021).

[17] Yonglong Xie, Andrew T. Pierce, Jeong Min Park, Daniel E. Parker, Eslam Khalaf, Patrick Ledwith, Yuan Cao, Seung Hwan Lee, Shaowen Chen, Patrick R. Forrester, Kenji Watanabe, Takashi Taniguchi, Ashvin Vishwanath, Pablo Jarillo-Herrero, and Amir Yacoby, Fractional Chern insulators in magic-angle twisted bilayer graphene, Nature (London) **600**, 439 (2021).

[18] Alexey I. Berdyugin *et al.*, Out-of-equilibrium criticalities in graphene superlattices, Science **375**, 430 (2022).

[19] Simon Turkel, Joshua Swann, Ziyan Zhu, Maine Christos, K. Watanabe, T. Taniguchi, Subir Sachdev, Mathias S. Scheurer, Efthimios Kaxiras, Cory R. Dean, and Abhay N. Pasupathy, Orderly disorder in magic-angle twisted trilayer graphene, Science **376**, 193 (2022).

[20] Tianye Huang, Xuecou Tu, Changqing Shen, Binjie Zheng, Junzhuan Wang, Hao Wang, Kaveh Khaliji, Sang Hyun Park, Zhiyong Liu, Teng Yang, Zhidong Zhang, Lei Shao, Xuesong Li, Tony Low, Yi Shi, and Xiaomu Wang, Observation of chiral and slow plasmons in twisted bilayer graphene, Nature (London) **605**, 63 (2022).

[21] Sergio C. de la Barrera, Samuel Aronson, Zhiren Zheng, Kenji Watanabe, Takashi Taniguchi, Qiong Ma, Pablo Jarillo-Herrero, and Raymond Ashoori, Cascade of isospin phase transitions in Bernal-stacked bilayer graphene at zero magnetic field, Nat. Phys. **18**, 771 (2022).

[22] Hyunjin Kim, Youngjoon Choi, Cyprian Lewandowski, Alex Thomson, Yiran Zhang, Robert Polski, Kenji Watanabe, Takashi Taniguchi, Jason Alicea, and Stevan Nadj-Perge, Evidence for unconventional superconductivity in twisted trilayer graphene, Nature (London) **606**, 494 (2022).

[23] Anna M. Seiler, Fabian R. Geisenhof, Felix Winterer, Kenji Watanabe, Takashi Taniguchi, Tianyi Xu, Fan Zhang, and R. Thomas Weitz, Quantum cascade of correlated phases in trigonally warped bilayer graphene, Nature (London) **608**, 298 (2022).

[24] Yuan Cao, Valla Fatemi, Shiang Fang, Kenji Watanabe, Takashi Taniguchi, Efthimios Kaxiras, and Pablo Jarillo-Herrero, Unconventional superconductivity in magic-angle graphene superlattices, Nature (London) **556**, 43 (2018).

[25] Matthew Yankowitz, Shaowen Chen, Hryhoriy Polshyn, Yuxuan Zhang, K. Watanabe, T. Taniguchi, David Graf, Andrea F. Young, and Cory R. Dean, Tuning superconductivity in twisted bilayer graphene, Science **363**, 1059 (2019).

[26] Xiaobo Lu, Petr Stepanov, Wei Yang, Ming Xie, Mohammed Ali Aamir, Ipsita Das, Carles Urgell, Kenji Watanabe, Takashi Taniguchi, Guangyu Zhang, Adrian Bachtold, Allan H. MacDonald, and Dmitri K. Efetov, Superconductors, orbital magnets and correlated states in magic-angle bilayer graphene, Nature (London) **574**, 653 (2019).

[27] Jeong Min Park, Yuan Cao, Kenji Watanabe, Takashi Taniguchi, and Pablo Jarillo-Herrero, Tunable strongly coupled superconductivity in magic-angle twisted trilayer graphene, Nature (London) **590**, 249 (2021).

[28] Zeyu Hao, A. M. Zimmerman, Patrick Ledwith, Eslam Khalaf, Danial Haie Najafabadi, Kenji Watanabe, Takashi Taniguchi, Ashvin Vishwanath, and Philip Kim, Electric field-tunable superconductivity in alternating-twist magic-angle trilayer graphene, Science **371**, 1133 (2021).

[29] Jeong Min Park, Yuan Cao, Li-Qiao Xia, Shuwen Sun, Kenji Watanabe, Takashi Taniguchi, and Pablo Jarillo-Herrero, Robust superconductivity in magic-angle multilayer graphene family, Nat. Mater. **21**, 877 (2022).

[30] Yiran Zhang, Robert Polski, Cyprian Lewandowski, Alex Thomson, Yang Peng, Youngjoon Choi, Hyunjin Kim, Kenji Watanabe, Takashi Taniguchi, Jason Alicea, Felix von Oppen, Gil Refael, and Stevan Nadj-Perge, Promotion of superconductivity in magic-angle graphene multilayers, Science **377**, 1538 (2022).

[31] Haoxin Zhou, Tian Xie, Takashi Taniguchi, Kenji Watanabe, and Andrea F. Young, Superconductivity in rhombohedral trilayer graphene, Nature (London) **598**, 434 (2021).

[32] Haoxin Zhou, Ludwig Holleis, Yu Saito, Liam Cohen, William Huynh, Caitlin L. Patterson, Fangyuan Yang, Takashi Taniguchi, Kenji Watanabe, and Andrea F. Young, Isospin magnetism and spin-polarized superconductivity in Bernal bilayer graphene, Science **375**, 774 (2022).

[33] Yiran Zhang, Robert Polski, Alex Thomson, Étienne Lantagne-Hurtubise, Cyprian Lewandowski, Haoxin Zhou, Kenji Watanabe, Takashi Taniguchi, Jason Alicea, and Stevan Nadj-Perge, Enhanced superconductivity in spin-orbit proximitized bilayer graphene, Nature (London) **613**, 268 (2023).

[34] Ludwig Holleis, Caitlin L. Patterson, Yiran Zhang, Heun Mo Yoo, Haoxin Zhou, Takashi Taniguchi, Kenji Watanabe, Stevan Nadj-Perge, and Andrea F. Young, Ising superconductivity and nematicity in Bernal bilayer graphene with strong spin orbit coupling, arXiv:2303.00742.

[35] Yuan Cao, Jeong Min Park, Kenji Watanabe, Takashi Taniguchi, and Pablo Jarillo-Herrero, Pauli-limit violation and re-entrant superconductivity in moiré graphene, Nature (London) **595**, 526 (2021).

[36] Jiang-Xiazi Lin, Phum Siriviboon, Harley D. Scammell, Song Liu, Daniel Rhodes, K. Watanabe, T. Taniguchi, James Hone, Mathias S. Scheurer, and J. I. A. Li, Zero-field superconducting diode effect in small-twist-angle trilayer graphene, Nat. Phys. **18**, 1221 (2022).

[37] Ethan Lake, Adarsh S. Patri, and T. Senthil, Pairing symmetry of twisted bilayer graphene: A phenomenological synthesis, Phys. Rev. B **106**, 104506 (2022).

[38] Folkert K. de Vries, Elías Portolés, Giulia Zheng, Takashi Taniguchi, Kenji Watanabe, Thomas Ihn, Klaus Ensslin, and Peter Rickhaus, Gate-defined Josephson junctions in magic-angle twisted bilayer graphene, Nat. Nanotechnol. **16**, 760 (2021).

[39] Daniel Rodan-Legrain, Yuan Cao, Jeong Min Park, Sergio C. de la Barrera, Mallika T. Randeria, Kenji Watanabe, Takashi Taniguchi, and Pablo Jarillo-Herrero, Highly tunable junctions and non-local Josephson effect in magic-angle graphene tunnelling devices, Nat. Nanotechnol. **16**, 769 (2021).

[40] J. Diez-Merida, A. Diez-Carlon, S. Y. Yang, Y. M. Xie, X. J. Gao, K. Watanabe, T. Taniguchi, X. Lu, K. T. Law, and Dmitri K. Efetov, Magnetic Josephson junctions and superconducting diodes in magic angle twisted bilayer graphene, arXiv:2110.01067.

[41] Ying-Ming Xie, Dmitri K. Efetov, and K. T. Law, Valley-polarized state induced φ_0-Josephson junction in twisted bilayer graphene, Phys. Rev. Res. **5**, 023029 (2023).

[42] Jin-Xin Hu, Zi-Ting Sun, Ying-Ming Xie, and K. T. Law, Valley polarization induced Josephson diode effect in twisted bilayer graphene, arXiv:2211.14846.

[43] Elías Portolés, Shuichi Iwakiri, Giulia Zheng, Peter Rickhaus, Takashi Taniguchi, Kenji Watanabe, Thomas Ihn, Klaus Ensslin, and Folkert K. de Vries, A tunable monolithic SQUID in twisted bilayer graphene, Nat. Nanotechnol. **17**, 1159 (2022).

[44] P. O. Sukhachov, Felix von Oppen, and L. I. Glazman, Andreev Reflection in Scanning Tunneling Spectroscopy of Unconventional Superconductors, Phys. Rev. Lett. **130**, 216002 (2023).

[45] B. D. Josephson, Possible new effects in superconductive tunnelling, Phys. Lett. **1**, 251 (1962).

[46] Manfred Sigrist and Kazuo Ueda, Phenomenological theory of unconventional superconductivity, Rev. Mod. Phys. **63**, 239 (1991).

[47] A. A. Golubov, M. Yu. Kupriyanov, and E. Il'ichev, The current-phase relation in Josephson junctions, Rev. Mod. Phys. **76**, 411 (2004).

[48] C. C. Tsuei, J. R. Kirtley, C. C. Chi, L. S. Yu-Jahnes, A. Gupta, T. Shaw, J. Z. Sun, and M. B. Ketchen, Pairing Symmetry and Flux Quantization in a Tricrystal Superconducting Ring of $Yba_2cu_3o_{7-\delta}$, Phys. Rev. Lett. **73**, 593 (1994).

[49] C. C. Tsuei and J. R. Kirtley, Pairing symmetry in cuprate superconductors, Rev. Mod. Phys. **72**, 969 (2000).

[50] Valentin Crépel, Tommaso Cea, Liang Fu, and Francisco Guinea, Unconventional superconductivity due to interband polarization, Phys. Rev. B **105**, 094506 (2022).

[51] Tommaso Cea and Francisco Guinea, Coulomb interaction, phonons, and superconductivity in twisted bilayer graphene, Proc. Natl. Acad. Sci. U.S.A. **118**, e2107874118 (2021).

[52] G. E. Blonder, M. Tinkham, and T. M. Klapwijk, Transition from metallic to tunneling regimes in superconducting microconstrictions: Excess current, charge imbalance, and supercurrent conversion, Phys. Rev. B **25**, 4515 (1982).

[53] F. Setiawan and Johannes Hofmann, Analytic approach to transport in superconducting junctions with arbitrary carrier density, Phys. Rev. Res. **4**, 043087 (2022).

[54] Cyprian Lewandowski, Étienne Lantagne-Hurtubise, Alex Thomson, Stevan Nadj-Perge, and Jason Alicea, Andreev reflection spectroscopy in strongly paired superconductors, Phys. Rev. B **107**, L020502 (2023).

[55] In the case of the f-wave superconductor, there is no restriction on the value of a given component of the spin, which can be $s_z = 0, \pm 1$.

[56] See Supplemental Material at http://link.aps.org/supplemental/10.1103/PhysRevLett.131.016003 for the equations of the STM tip-superconductor junction; a discussion about the subgap conductance of the junction, in which we compare s- and f-wave superconductors and include an analytical derivation of the Andreev states due to tip-induced intervalley scattering in the f-wave case; the critical current of Josephson junctions compared to experiments; details of the Josephson junction model; a toy model mixed junction and additional Andreev spectra, which includes Refs. [57–61].

[57] Pilkyung Moon, Young-Woo Son, and Mikito Koshino, Optical absorption of twisted bilayer graphene with interlayer potential asymmetry, Phys. Rev. B **90**, 155427 (2014).

[58] Rafi Bistritzer and Allan H. MacDonald, Moiré bands in twisted double-layer graphene, Proc. Natl. Acad. Sci. U.S.A. **108**, 12233 (2011).

[59] Enrico Perfetto, Gianluca Stefanucci, and Michele Cini, Equilibrium and time-dependent Josephson current in one-dimensional superconducting junctions, Phys. Rev. B **80**, 205408 (2009).

[60] A. Yu Kitaev, Unpaired Majorana fermions in quantum wires, Phys. Usp. **44**, 131 (2001).

[61] Chikara Ishii, Josephson currents through junctions with normal metal barriers, Prog. Theor. Phys. **44**, 1525 (1970).

[62] P. W. Anderson, Theory of dirty superconductors, J. Phys. Chem. Solids **11**, 26 (1959).

[63] Xianqing Lin and David Tománek, Minimum model for the electronic structure of twisted bilayer graphene and related structures, Phys. Rev. B **98**, 081410(R) (2018).

[64] Francisco Guinea and Niels R. Walet, Electrostatic effects, band distortions, and superconductivity in twisted graphene bilayers, Proc. Natl. Acad. Sci. U.S.A. **115**, 13174 (2018).

[65] Louk Rademaker, Dmitry A. Abanin, and Paula Mellado, Charge smoothening and band flattening due to Hartree corrections in twisted bilayer graphene, Phys. Rev. B **100**, 205114 (2019).

[66] L. A. Gonzalez-Arraga, J. L. Lado, Francisco Guinea, and Pablo San-Jose, Electrically Controllable Magnetism in Twisted Bilayer Graphene, Phys. Rev. Lett. **119**, 107201 (2017).

[67] Javad Vahedi, Robert Peters, Ahmed Missaoui, Andreas Honecker, and Guy Trambly de Laissardière, Magnetism of magic-angle twisted bilayer graphene, SciPost Phys. **11**, 083 (2021).

[68] Héctor Sainz-Cruz, Tommaso Cea, P. A. Pantaleón, and Francisco Guinea, High transmission in twisted bilayer graphene with angle disorder, Phys. Rev. B **104**, 075144 (2021).

[69] We use a commensurate lattice, but we caution that incommensurability has an impact on transport [70].

[70] Miguel Gonçalves, Hadi Z. Olyaei, Bruno Amorim, Rubem Mondaini, Pedro Ribeiro, and Eduardo V. Castro, Incommensurability-induced sub-ballistic narrow-band-states in twisted bilayer graphene, 2D Mater. **9**, 011001 (2021).

[71] F. D. M. Haldane, Model for a Quantum Hall Effect Without Landau Levels: Condensed-Matter Realization of the "Parity Anomaly", Phys. Rev. Lett. **61**, 2015 (1988).

[72] To induce a superconducting gap of magnitude Δ, the necessary amplitudes are $\Delta_S = \Delta/2$ for s-wave, $\Delta_K = \Delta/4$ for Kitaev, and $\Delta_F \approx \Delta/(6\sqrt{3})$ for f-wave pairing.

[73] In SIS junctions with the leads at $n = +2.4$ (-2.4), the chemical potential of the link is placed in the middle of the gap between the flat bands and the holelike (electronlike) remote bands.

[74] Vinay Ambegaokar and Alexis Baratoff, Tunneling Between Superconductors, Phys. Rev. Lett. **10**, 486 (1963).

[75] M. Alvarado and A. L. Yeyati, Transport and spectral properties of magic-angle twisted bilayer graphene junctions based on local orbital models, Phys. Rev. B **104**, 075406 (2021).

[76] Alexandre M. Zagoskin, The half-periodic Josephson effect in an s-wave superconductor—normal-metal—d-wave superconductor junction, J. Phys. Condens. Matter **9**, L419 (1997).

[77] L. N. Bulaevskii, V. V. Kuzii, and A. A. Sobyanin, Superconducting system with weak coupling to the current in the ground state, JETP Lett. **25** (1977).

[78] Alex Zazunov and Reinhold Egger, Supercurrent blockade in Josephson junctions with a Majorana wire, Phys. Rev. B **85**, 104514 (2012).

[79] Mathias S. Scheurer and Rhine Samajdar, Pairing in graphene-based moiré superlattices, Phys. Rev. Res. **2**, 033062 (2020).

[80] Jacob Linder, Annica M. Black-Schaffer, Takehito Yokoyama, Sebastian Doniach, and Asle Sudbø, Josephson current in graphene: Role of unconventional pairing symmetries, Phys. Rev. B **80**, 094522 (2009).

[81] Hubert B. Heersche, Pablo Jarillo-Herrero, Jeroen B. Oostinga, Lieven M. K. Vandersypen, and Alberto F. Morpurgo, Bipolar supercurrent in graphene, Nature (London) **446**, 56 (2007).

[82] Dingran Rui, Luzhao Sun, N. Kang, Hailin Peng, Zhongfan Liu, and H. Q. Xu, Superconductivity in an al-twisted bilayer graphene-al junction device, Jpn. J. Appl. Phys. **59**, SGGI07 (2020).

[83] Prathyush P. Poduval and Mathias S. Scheurer, Vestigial singlet pairing in a fluctuating magnetic triplet superconductor: Applications to graphene moiré systems, arXiv:2301.01344.

Correction: The previously published Fig. 4 contained an error and has been replaced.